EG&G Idaho, Inc.

FORM EG&G-398
(Rev. 11-79)

INTERIM REPORT

Accession No. _____

Report No. EGG-CDAP-5216

Contract Program or Project Title: Fuel Behavior Model Development

Subject of this Document: Cladding Creep (CCSTRN and CCSTRS)

Type of Document: Interim Report

Author(s): D. L. Hagrman

Date of Document: July 1980

Responsible NRC Individual and NRC Office or Division: G. P. Marino

EG&G Idaho, Inc.
Idaho Falls, Idaho 83415

Prepared for the
U.S. Nuclear Regulatory Commission
Washington, D.C.
Under DOE Contract No. DE-AC07-76ID01570
NRC FIN No. A6050

INTERIM REPORT

CONTENTS

LIST OF FIGURES

LIST OF TABLES

FOREWORD

This report describes a revised model for cladding creepdown under compressive stress. The report will become part of an update to the current Materials Properties (MATPRO) Handbook[a] used in the fuel rod behavior modeling task performed at the INEL.

This revision to the previous MATPRO cladding creepdown model incorporates the results of the HOBBIE-1 in-reactor experiment to deduce a preliminary model for cladding creep under compressive stress. The model is an interim result because expected results from the HOBBIE-2 through HOBBIE-8 experiments are not yet available. However, uncertainty estimates have been provided for both the predicted creep strain increment and the stress deduced from a given creep strain increment.

The format and numbering scheme used in this report are consistent with its intended use as an update to the MATPRO handbook. Readers who require descriptions of the rest of the material properties package or of the use of this package should consult the code descriptions[a,b,c].

---

a D. L. Hagrman, G. A. Reymann, and R. E. Mason, MATPRO-Version 11 Revision 1: A Handbook of Materials Properties for Use in the Analysis of Light Water Reactor Fuel Rod Behavior, NUREG/CR-0497 TREE-1280, Rev 1, (February 1980).

b G. A. Berna et al., FRAPCON-1: A Code for the Steady-State Analysis of Oxide Fuel Rods, CDAP-TR-78-032-R1, (November 1978).

c L. J. Siefken et al., FRAP-T5: A Computer Code for the Transient Analysis of Oxide Fuel Rods, NUREG/CR-0840 TREE-1281, (June 1979).

7. CLADDING CREEP (CCSTRN AND CCSTRS)

(D. L. Hagrman)

Cladding creep due to coolant pressure during steady state operation is important in modeling the size of the fuel-cladding gap and thus the initial stored energy at the start of transients. For fuel rods with low internal pressure, the creep may be sufficiently rapid to also affect fuel relocation and the effective conductivity of fuel pellets. Subcodes for finding creep strain as a function of stress and the stress required to produce a given creep strain are presented in this section. The model used in these subcodes is based primarily on surface displacement data from the HOBBIE-1 test conducted by the U.S. Nuclear Regulatory Commission and the Energieonderzock Centrum Nederland.

7.1 Summary

The basic equation used in both the CCSTRN and CCSTRS subroutines is

$$\dot{\varepsilon}(t) = B\,A - \int_0^t B \exp\left(-[t-t']\left[\frac{\phi}{\Psi} + \frac{1}{\tau}\right]\right) \dot{\varepsilon}(t')\,dt' \qquad \text{(B-7.1)}$$

where

$\dot{\varepsilon}(t)$ = tangential component of creep strain rate (s^{-1})

t = time since creep strain was zero (s)

ϕ = fast neutron flux (neutrons/(m^2-s)), E > 1 MeV

Ψ = correlation fluence, given by Equation B-7.4 (neutrons/m^2), E > 1 MeV

τ = zero flux correlation time, given by Equation B-7.5 (s)

A = ultimate strain for infinite correlation (unitless), given by Equation B-7.2

B = a rate constant (s^{-1}), given by Equation B-7.3.

Correlations for the parameters A and B were obtained from out-of-pile creep strain versus time data. The expressions are

$$A = 3.83 \times 10^{-19} |\sigma|^{r} \frac{\sigma}{|\sigma|} \qquad \text{(B-7.2)}$$

$$B = 4.69 \times 10^{-6} |\sigma|^{r} \exp\left(\frac{-25100}{T}\right), \text{ for } T \geq 615K$$

$$1.9519804 \times 10^{-16} |\sigma|^{r} \exp\left(\frac{-10400}{T}\right), \text{ for } T < 615K \qquad \text{(B-7.3)}$$

where

σ = tangential component of stress (Pa)

T = temperature (K). Input temperatures are limited to the range 450 to 750K

r = 2.0 for stress between -0.2 and -0.75 times the strength coefficient of the cladding
= 0.5 for stress between 0 and -0.2 times the strength coefficient of the cladding
= 25.0 for stress less than -0.75 times the strength coefficient of the cladding. The strength coefficient is approximated by the linear expression $1.5 \times 10^{9} - 1.5 \times 10^{6}$ T and the constants in Equation (B-7.3) are modified when stress is outside the range -0.2 to -0.75 times the strength coefficient in order to guarantee continuity at the boundaries of this range.

Preliminary expressions for the correlation fluence, Ψ, and zero flux correlation time, τ, were obtained from the slope of secondary creep rates versus temperature under tensile stress. These expressions are

$$\Psi = \begin{cases} 2.9 \times 10^{6} \exp\left(\frac{25100}{T}\right), & \text{for } T \geq 615K \\ 6.967795 \times 10^{16} \exp\left(\frac{10400}{T}\right), & \text{for } T < 615K \end{cases} \quad \text{(B-7.4)}$$

$$\tau = \begin{cases} 8.6 \times 10^{-11} \exp\left(\frac{25100}{T}\right), & \text{for } T \geq 615K \\ 2.0663116 \exp\left(\frac{10400}{T}\right), & \text{for } T < 615K \end{cases} \quad \text{(B-7.5)}$$

The CCSTRN subroutine calculates the tangential component of cladding creep strain at the end of a time step with constant cladding temperature, flux and stress. For time step intervals less than a time to steady state, the infinite-correlation approximation[a] is used to integrate Equation (B-7.1). The resultant expression for creep strain is

$$\varepsilon_{final} = [A - \varepsilon_{boundary}] [1 - \exp(-B\Delta t)] + \varepsilon_{initial} \quad \text{(B-7.6)}$$

where

ε_{final} = tangential component of creep strain at the end of the time step (unitless)

$\varepsilon_{initial}$ = tangential component of creep strain at the start of the time step (unitless)

$\varepsilon_{boundary}$ = a boundary condition parameter used to force the creep rate to be continuous at the time step boundary when temperature and stress do not change (unitless). This parameter is zero for the first time step and is determined by Equation (B-7.26) for subsequent time steps

Δt = time step duration (s).

---

[a] The exponent in Equation (B-7.1) is approximated by a one.

For time step durations longer than the time to steady state, the steady state approximation ($\ddot{\varepsilon}$ (t) ≈ 0) is used to integrate Equation (B-7.1). The resultant expression for creep strain is

$$\varepsilon_{final} = [A - \varepsilon_{boundary}] [1 - \exp(-B\,\Delta t_{ss})] + \frac{BA\,[\Delta t - \Delta t_{ss}]}{1 + \frac{\phi}{\Psi} + \frac{1}{\tau}} + \varepsilon_{initial} \qquad \text{(B-7.7)}$$

where Δt_{ss} = the time to steady state(s).

The time to steady state is defined to be the time when the creep strain rate given by Equations (B-7.6) and (B-7.7) are equal.

$$\Delta t_{ss} = \begin{cases} -\frac{1}{B} \ln \left[\frac{A}{1 + \frac{B}{\frac{\phi}{\Psi} + \frac{1}{\tau}}} \; \frac{1}{[A - \varepsilon_{boundary}]} \right] \\ 0 \text{ if the argument of the log term is outside the range } 0 < \text{argument} < 1 \end{cases} \qquad \text{(B-7.8)}$$

The CCSTRS subroutine uses an interaction technique and trial assumptions to solve Equation (B-7.6) or (B-7.7) for stress when ε_{final}, $\varepsilon_{initial}$, and Δt are known. The procedure begins by solving Equation (B-7.6) with the implied assumption that Δt is less than Δt_{ss}. In this case, the possible range of stresses is bounded and the function is monotonic. The range is cut in half in each of several iterations by testing the stress at the midpoint of the possible range. If substitution of the trial solution into Equation (B-7.8) yields a Δt_{ss} which is longer than Δt, the trial solution is adopted.

A second trial solution is obtained by solving Equation (B-7.7) for $|\sigma|^r$ with the assumption Δt_{ss} is zero. If this trial solution yields $\Delta t_{ss} = 0$ in Euqation (B-7.8), it is adopted.

If neither of the two trial solutions are adopted, the technique used in the CCSTRS subroutine employs the observation that the first

provides a maximum $|\sigma|^r$, and the second trial solution provides a minimum initial slope. The implied range of possible stress is then cut in half in each of several iterations by testing in Equations (B-7.8) and (B-7.7) with the stress at the midpoint of the range.

Uncertainty estimates for the creep strain and stress are provided by the CCSTRN and CCSTRS subroutines. Both estimates are based on the observation that the only creep data with compressive stresses are at a temperature of 644 K and stresses in the range -120 to -140 MPa. The expression used to estimate the uncertainty of the strain calculated in the CCSTRN subroutine is

$$f_{\varepsilon+} = 1 + 0.3 \left(1 + 2 \left|\frac{\sigma + 130 \times 10^6}{130 \times 10^6}\right| + 5 \left|\frac{T - 644}{644}\right|\right) \qquad \text{(B-7.9a)}$$

$$f_{\varepsilon-} = 0.4 \,/\, \left(1 + 2 \left|\frac{\sigma + 130 \times 10^6}{130 \times 10^6}\right| + 5 \left|\frac{T - 644}{644}\right|\right) \qquad \text{(B-7.9b)}$$

where $f_{\varepsilon\pm}$ are the upper and lower uncertainty estimates of the calculated creep strain increment magnitude expressed as a fraction of the calculated creep strain increment magnitude.

The expression used to estimate the uncertainty of the stress calculated in the CCSTRS subroutine is

$$f_{\sigma+} = 1 + 0.075 \left(1 + 2 \left|\frac{\sigma + 130 \times 10^6}{130 \times 10^6}\right| + 5 \left|\frac{T - 644}{644}\right|\right) \qquad \text{(B-7.10a)}$$

$$f_{\sigma-} = 0.85 \,/\, \left(1 + 2 \left|\frac{\sigma + 130 \times 10^6}{130 \times 10^6}\right| + 5 \left|\frac{T - 644}{644}\right|\right) \qquad \text{(B-7.10b)}$$

where $f_{\sigma\pm}$ are the upper and lower uncertainty estimates of the calculated stress magnitude expressed as a function of the calculated stress magnitude.

The following subsections discuss available data and development of the model. Section B-7.5 contains a listing of the CCSTRN and CCSTRS subcodes and references are provided in Section B-7.6.

7.2 Survey of Available Data

At the present time, data which measure creep under tensile stress are being supplemented by data for creep with compressive stress in very limited ranges of temperature and stress. The available theories and data for creep under compressive stress are surveyed in this section. Additional references from the extensive literature on tensile creep experiments are provided in a bibliography.

At the present time, there are no theories directed specifically at compressive stress but Dollins and Nichols[B-7.1], Piercy[B-7.2], MacEwen[B-7.3], and Nichols[B-7.4, B-7.5] have discussed similar physical models which explain the general features of in-pile creep of cladding under tensile stress. For the temperature range 523 to 623 K, these authors believe the controlling mechanism for in-pile creep at stresses below 70 to 100 MPa is the preferred alignment of irradiation-induced dislocation loops during nucleation. At higher stresses, the effective stress at dislocations is thought to be sufficiently large to allow dislocation glide between the neutron produced depleted zones. The creep rate would then be controlled by the combined rates of dislocation glide between depleted zones and climb out of these zones. Although some of Nichol's ideas have been challenged[B-7.5, B-7.6, B-7.7], the predicted linear stress dependence of strain rate at low stress is supported by several authors[B-7.8, B-7.9] and his prediction that the strain rate at high stress is proportional to approximately the one-hundreth power of stress in the 523 to 623 K temperature range is consistent with the MATPRO models for cladding plastic deformation at high stress[a]. Unfortunately, Nichols predicts a complex relation between strain rate and stress for intermediate stress. The dependence of strain rate on stress is expected to vary from the tenth power of stress to the first power and then to the fourth power as stress increases. The physical model proposed by Nichols has been consulted but not used directly because the cost associated with the use of such a detailed model is not justified until compressive creep data confirms the model.

---

[a] The MATPRO models for cladding plastic deformation, CSTRES, CSTRAN, and CSTRNI are described in Appendix B.8 of the MATPRO-11 handbook; D. L. Hagrman, G. A. Reymann, R. E. Mason, MATPRO-Version 11 (Revision 1), A Handbook of Materials Properties for Use in the Analysis of Light Water Reactor Fuel Rod Behavior, NUREG/CR-0497 TREE-1280, Rev. 1 (February 1980).

A similar, but less physically founded stress dependence is proposed by Fidleris in his review of experimental data[B-7.9]. He reported that creep rate varies linearly with stress at temperatures around 570 K and stresses less than one third the yield stress. With increasing stress, the strain rate is reported to be proportional to higher powers of stress, reaching a power of 100 at stresses of 600 MPa. The model for creep-down to be developed in the next section will use only the general features of the stress dependence reported by Fidleris because insufficient creep-down data exist to support detailed modeling at this time.

The data referenced by Fidleris show the in-reactor creep rate depends on material, flux temperature and direction of testing as well as stress. At temperatures below half the melting temperature (1050 K) and stresses lower than the yeild stress, the in-reactor creep reaches a constant rate while the out-of-reactor creep rate becomes negligibly small with time. The steady state creep rate is stated to be independent of test history or strain, at least for fast neutron fluences below 3×10^{24} neutrons/m^2 ($E > 1$ MeV).

Below 450 K, temperature is reported to have little effect and, for stresses below the yield stress, the strain is less than 0,001. The out-of-reactor creep data of Fidleris can be described by

$$\varepsilon = A \log t + B \qquad \text{(B-7.11)}$$

where

ε = strain

t = time

A,B = constants.

In the range 450 to 800 K, Fidleris reports that the out-of-reactor creep strain is often represented by equations of the type

$$\varepsilon = At^m + B \qquad \text{(B-7.12)}$$

where, E, t, A and B were defined in conjunction with Equation (B-7.11) and m is a constant between zero and one. Recovery of some of the strain is possible in this temperature range and dynamic strain aging[B-7.10] frequently causes anomalously low creep strains and rates.

Equations (B-7.11) and (B-7.12) and the other conclusions in Fidleris' review are based on his own extensive data for uniaxial, tensile creep of zirconium alloys, both in and out-of-reactor[B-7.11]. From these data he has concluded that the in-reactor creep is approximately proportional to the fast neutron flux for all temperatures. Other investigators treat the effect of fast neutron flux on creep in different ways. Although most authors have treated in-reactor creep as the sum of the out-of-reactor creep and an additional irradiation-induced creep proportional to fast neutron flux to some power a, there is disagreement about the magnitude of the exponent a. Ross-Ross and Hunt[B-7.8], report that creep rate is directly proportional to the fast flux, Wood[B-7.13, B-7.14] uses a = 0.85, Kohn[B-7.15] uses a = 0.65 and Gilbert[B-7.16] finds a = 0.5 for yielding creep at moderate stress levels. MacEwin[B-7.3] and Nichols[B-7.4] have resolved this apparent conflict by suggesting the flux exponent can have values from 0 (Nichols) or 0.5 (MacEwin) to 1.0, depending on the flux and temperature.

The expressions for calculating creep-down which will be developed in the next section will model the effect of fast neutron flux on creep with an expression which is proportional to fast neutron flux for large fluxes but less dependent on flux for smaller fluxes. Equation (B-7.12), Fidleris' equation for creep strain versus time with tensile stress, will not be used because it is inconsistent with data obtained from tests with compressive stress.

The effects of grain size annealing and texture are addressed by several authors. Fidleris finds that the Zircaloy-2 creep rate increases continuously with grain size at 573 K. However, within the limited range

of grain sizes formed in his recrystallized Zircaloy-2 (6 to 20 μm) very little variation is reported. Stehle[B-7.17] reports creep strains in cold worked material which are more than twice as large as the creep strains in recrystallized cladding. He also reports that the short time creep strain of stress relieved tubes is larger than that of recrystallized tubes, but that the plots of creep strain versus time for the stress relieved and recrystallized cladding intersect at about 6,000 hours. Kohn[B-7.15] reported that the biaxial creep rate of Zr-2.5Nb fuel cladding is about 10 times higher than that of pressure-tube material under similar conditions. He states that texture differences between the materials and the overaged precipitate structure in the as-manufactured cladding can explain the difference in creep rates. The importance of texture is disputed by Stehle[B-7.17] who reported that the mechanical anisotropy (especially in long time creep) is surprisingly low compared to the anisotropy in short time creep at room temperature. The effects of grain size, annealing and texture will not be considered in the creep-down model developed in the next section because an explicit model for these effects on creepdown would be premature at this time.

The theories surveyed above may be misleading when applied to compressive creep because they are based primarily on tensile stress data. Picklesimer[B-7.18], Lucas and Bement[B-7.19] and Stehle[B-7.17] have pointed out that deformation with compressive stress differs from tensile compression. Stehle has obtained data showing that the magnitude of the creep strain of tubes under external pressure can be as small as half the creep strain of tubes under internal pressure.

The biaxial compressive stress data now available include out-of-reactor measurements at three stresses and one temperature. Results from a single in-reactor experiment are also available. All but one of the experiments were conducted by Hobson using tubes from a shipment of typical pressurized water reactor cladding purchased specifically for use in fuel cladding research programs sponsored by the Division of Reactor Safety Research, Nuclear Regulatory Commission[B-7.20].

The only biaxial compressive strain data from a different lot of cladding were reported by Stehle[B-7.17]. His measurements of the tangential creep as a function of time for standard stress-relieved tubing fabricated according to KWU (Kraftwerke Union) specifications are reproduced in Figure B-7.1. The tangential stress in this test was 140 MPa and the temperature was 643 K. The magnitude of the measured creep strains are somewhat smaller than the out-of-pile strains computed in the next section from Hobson's out-of-pile data at the same temperature, but within the range of the scatter reported by Stehle for cladding with varying cold work and stress relief annealing histories. Since the details of the stress relief anneal on the lot of cladding used by Stehle are not reported, the data will be used only to assess the uncertainty of the creep-down model.

The data reported by Hobson[B-7.21 - B-7.24] are radial displacements of the cladding surface at various azimuthal angles and axial positions (6.34 mm apart). The twenty probes used to measure the displacement were arranged in a double helix pattern over a 50.8 mm length of cladding as shown by probe number in Table B-7.1. This table is arranged so that the location of the probes may be visualized by thinking of the cladding surface as split along the cylinder axis and "rolled out" in the plane of the page. Hobson has pointed out[B-7.23] that the exact shape of the cladding surface cannot be determined with point-by-point data from a few radial probes and that the exact stress state at any point in the sample is related to the geometry of the sample. In spite of these complications, the data can be analyzed to obtain the average tangential strain as discussed in the next section of this report. The Hobson data play a dominant role in the development of the creep-down model because the cladding is typical of light water reactor cladding, the stress is compressive, the cladding displacement is reported as a function of time at two hour intervals, and the temperature is typical of the cladding temperatures predicted by the FRAPCON-2 code. The only atypical feature of the data is the magnitude of the stresses employed by Hobson, 125 and 135 MPa. These stresses are characteristic of low pressure rods so extrapolation to smaller stress magnitudes is necessary to model current fuel rod prepressurization levels.

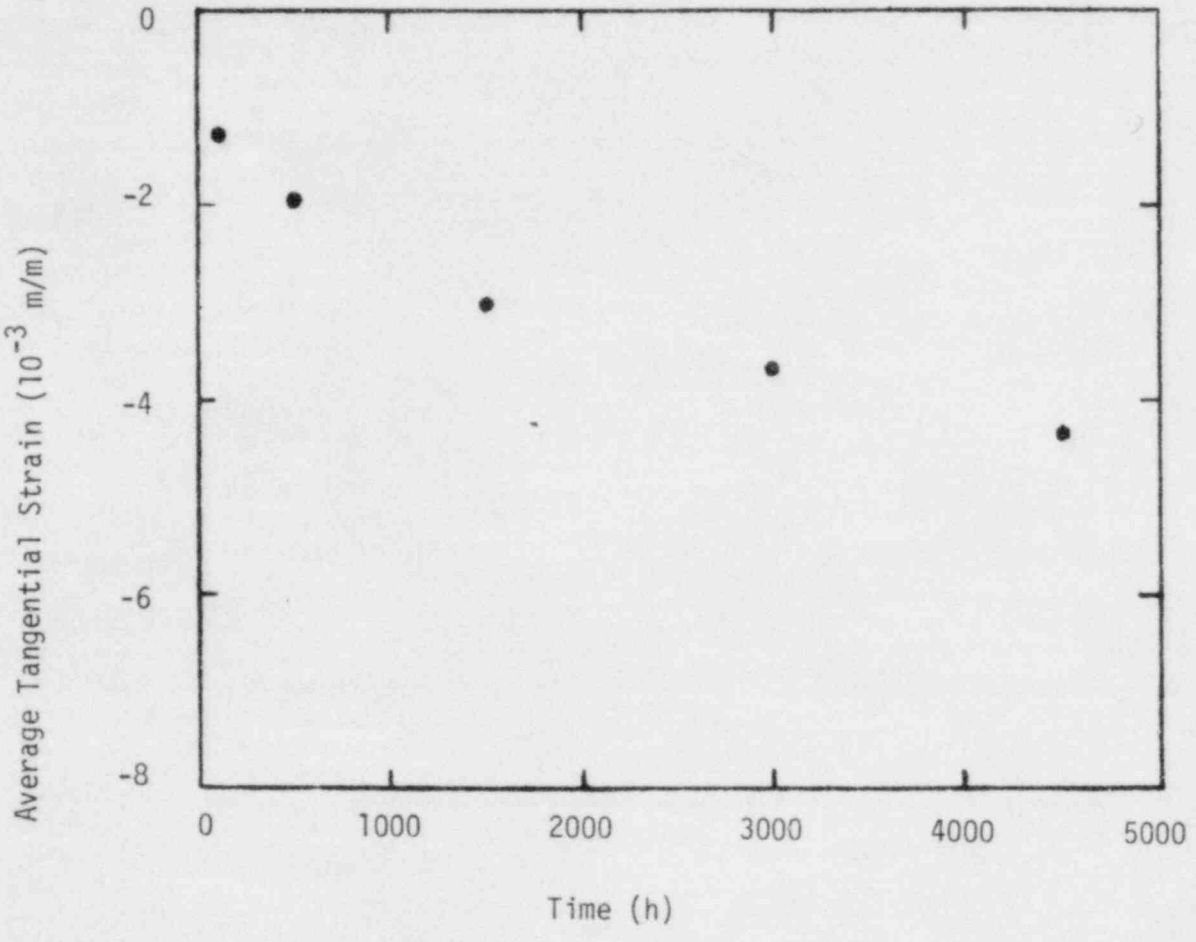

Fig. B-7.1 Average tangential creep strain as a function of time at 140 MPa and 643 K reported by Stelle[B-7.17].

TABLE B-7.1

SURFACE COORDINATES OF PROBES WHICH MEASURE
RADIAL DISPLACEMENT

Axial Position (mm)	Azimuthal Angle (Degrees)							
	0	45	90	135	180	225	270	315
0.00	1	--	--	--	13	--	--	--
6.35	--	4	--	--	--	16	--	--
12.70	--	--	7	--	--	--	19	--
19.05	--	--	--	10	--	--	--	22
25.40	2	--	8	--	14	--	20	--
31.75	--	5	--	--	--	17	--	--
38.10	--	--	9	--	--	--	21	--
44,45	--	--	--	11	--	--	--	23
50.80	3	--	--	--	15	--	--	--

7.3 Development of the Model

In the last section it was concluded that the most relevant data for modeling cladding creep down under the compressive stress of steady state LWR reactor conditions are the data of Hobson. Extensive theory and tensile creep data are useful only to provide a tentative extension of the model to stresses and temperatures where no creepdown data are available.

The first step in the analysis of Hobson's data was to estimate the average tangential strain from radial displacements measured by probes at the locations shown in Table B-7.I of Section 7.2. This was done by inspecting plots of the radial displacement measured for each test. Table B-7.II and Figure B-7.2 are an example of the results. The table was constructed from Hobson's data for Test 269-4 (14.48 MPa pressure) at 200 hours and the figure is a polar plot of the radial displacement as a function of the azimuthal angle of the probe. The plot exaggerates the radial displacement by a factor of ten compared to the scale of the circle which represents zero displacement. From an inspection of the figure it can be seen that the radial displacements at 200 hours in Test 269-4 are consistent with the assumption that the cladding surface was an ellipse with major axis between 0° and 45° and the center of the ellipse displaced slightly toward the 180 to 270° quadrant. There is some variation with axial position, as shown by the scatter in the displacements with common azimuthal angles and different axial positions.

The elliptical shape and gradual axial variations are also consistent with general descriptions of cladding surfaces after creepdown given by Stehle[B-7.25] and Bauer[B-7.26]. On the basis of several plots like Figure B-7.2 and the general descriptions just mentioned, the

TABLE B-7.II

RADIAL DISPLACEMENTS AT 200 HOURS IN TEST 269-4[a] (10^{-3} mm)

Axial Position (mm)	Azimuthal Angle (Degrees)							
	0	45	90	135	180	225	270	315
0.00	4	--	--	--	12	--	--	--
6.35	--	6	--	--	--	12	--	--
12.70	--	--	48	--	--	--	12	--
19.05	--	--	--	-19	--	--	--	-29
25.40	31	--	-63	--	40	--	-58	--
31.75	--	3	--	--	--	31	--	--
38.10	--	--	-77	--	--	--	-60	--
44.45	--	--	--	-36	--	--	--	-38
50.80	31	--	--	--	32	--	--	--

[a] 14.48 MPa pressure differential and 0.127 mm pellet-cladding gap[B-7.23].

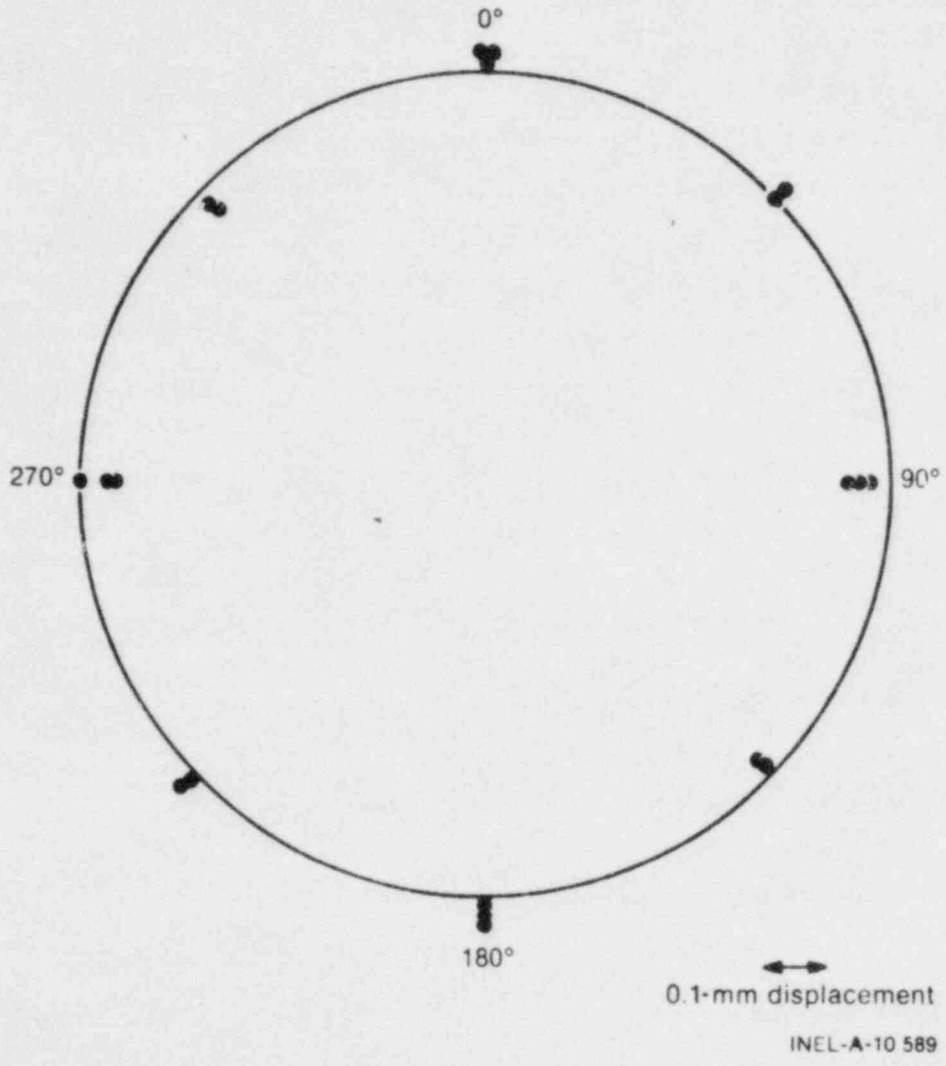

Fig. B-7.2 Radial displacement of cladding surface at 200 hours in Test 269-4.

author has concluded (a) an ellipse is a reasonable approximation for the cladding surface at any given height prior to extensive fuel-cladding interaction and (b) the major and minor axis (length or orientation or both) vary slowly with axial position.

The assumption that the cladding surface at any axial position is an ellipse allows calculation of the average tangential strain as outlined in the six steps below.

(1) The circumference of the elliptical surface was related to the major and minor semi-axis lengths with the approximate expression

$$c = 2\pi\sqrt{\frac{a^2 + b^2}{2}} \quad . \qquad \text{(B-7.13)}$$

where

c = circumference (m)

a,b = semi-axis lengths (m).

(2) The average tangential strain was defined as

$$\varepsilon_\theta = \int_{\text{circumference}} \frac{ds}{s} \approx \frac{c_{final} - c_{initial}}{c_{initial}} \qquad \text{(B-7.14)}$$

where

s = arc length (m)

ε_θ = average tangential strain (unitless)

$c_{initial}$ = initial circumference (m)

c_{final} = final circumference (m)

(3) Equations (B-7.13) and (B-7.14) were combined to obtain

$$\varepsilon_\theta \simeq \sqrt{\frac{a_{final}^2 + b_{final}^2}{a_{initial}^2 + b_{initial}^2}} - 1. \qquad \text{(B-7.15)}$$

(4) $a_{initial}$ and $b_{initial}$ were assumed equal to r_o and a_{final} and b_{final} were set equal to the initial values plus Δa and Δb.

(5) A Taylor series expansion to order $\frac{\Delta a}{r_o}$ and $\frac{\Delta b}{r_o}$ was used with Equation (B-7.15) and Step (4) to find

$$\varepsilon_\theta \simeq \frac{1}{2}\left(\frac{\Delta a + \Delta b}{r_o}\right) \qquad \text{(B-7.16)}$$

where

r_o = initial radius of the outside (circular) surface of the cladding (m)

$\Delta a, \Delta b$ = change of the major and minor semi-axes lengths (m).

(6) Measurements of the radial displacements at one axial position (25.4 mm) and azimuthal angles of 0°, 90°, 180°, and 270° are available from Hobson's data. If these four measurements happen to occur along the major and minor axes of the ellipse, Equation (B-7.16) is sufficient to convert the data to an expression for the average circumferential component of the strain. When the radial displacements at 25.4 mm are not measured along the major and minor axes of the ellipse, the derivation is more complex but the result

(to order $\frac{\Delta a}{r_o}$ and $\frac{\Delta b}{r_o}$ in the Taylor series expansion) is an equation of the same form as Equation (B-7.16) with Δa and Δb replaced by the average radial displacements along any two axes at right angles to each other and at any angle to the major and minor axes of the ellipse. That is

$$\varepsilon_\theta \simeq \frac{1}{2}\left(\frac{\Delta a' + \Delta b'}{r_o}\right) \qquad \text{(B-7.17)}$$

where

$\Delta a', \Delta b'$ = change of the cladding radius measured along any mutually perpendicular axes at one axial position (m).

The second part of the analysis of Hobson's data was to describe the average tangential strains obtained from the data and Equation (B-7.17). Figure B-7.3 displays the calculated average tangential strain from two out-of-pile tests at 15.86 MPa differential pressure. During the first 600 hours, the strains are remarkably consistent. During the last 400 hours of the tests, the strain in Test 269-27 was noticably larger than that of Test 269-8. Test 269-27 had a large simulated axial gap centered about the axial position of the four probes used to determine the strain. Test 269-8 had only a small axial gap. The difference in strain at long times is probably due to the effect of the different contact times with the simulated fuel.

Figure B-7.4 illustrates the strain versus time results obtained from the one 14.48 MPa out-of-pile test. The magnitude of the strain at any time is significantly smaller than the strains obtained with the 15.86 MPa tests.

In an effort to describe the strain versus time data shown in Figures B-7.3 and B-7.4, the constants in Fidleris' equations for tensile creep (Equations (B-7.11 and B-7.12)) were fit to selected strain-time pairs. Each equation was then tested by extrapolating to longer or shorter

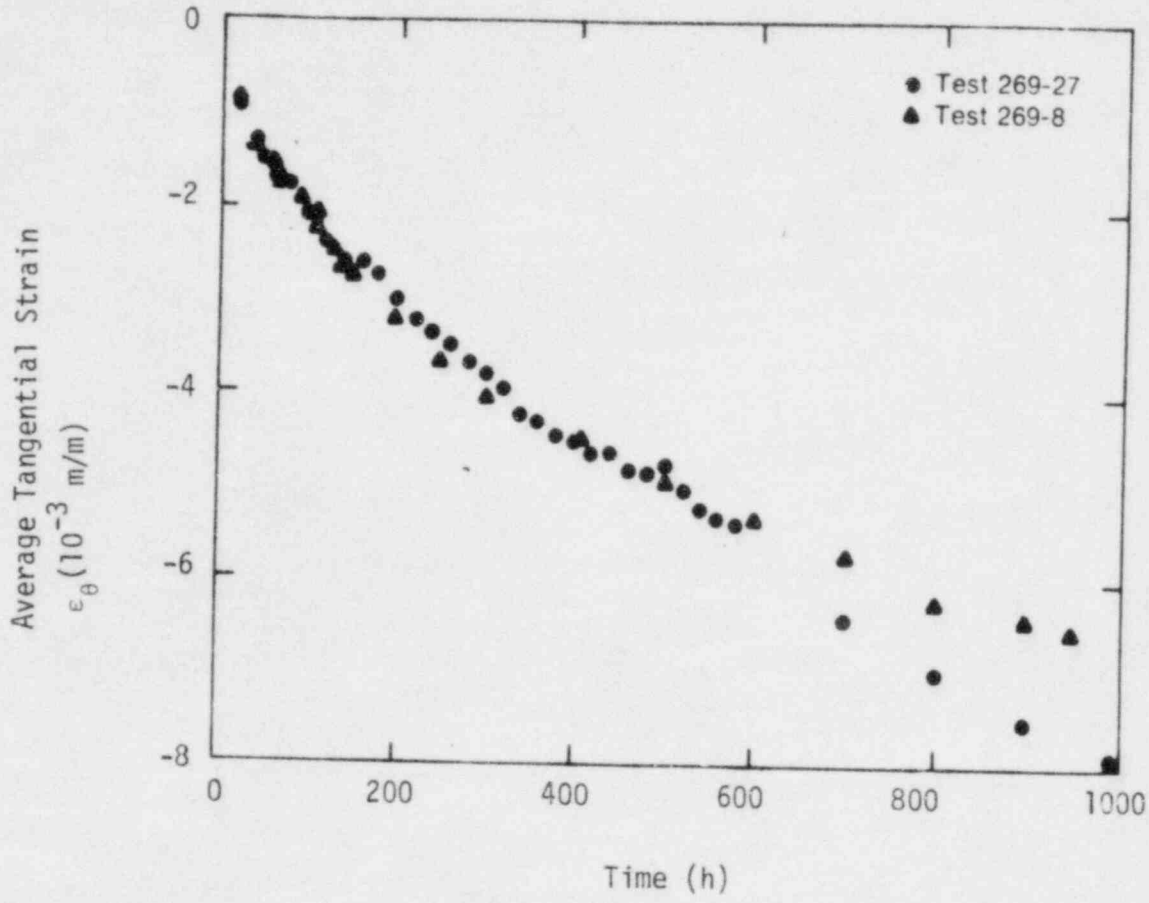

Fig. B-7.3 Average tangential strain as a function of time at 14.86 MPa differential pressure.

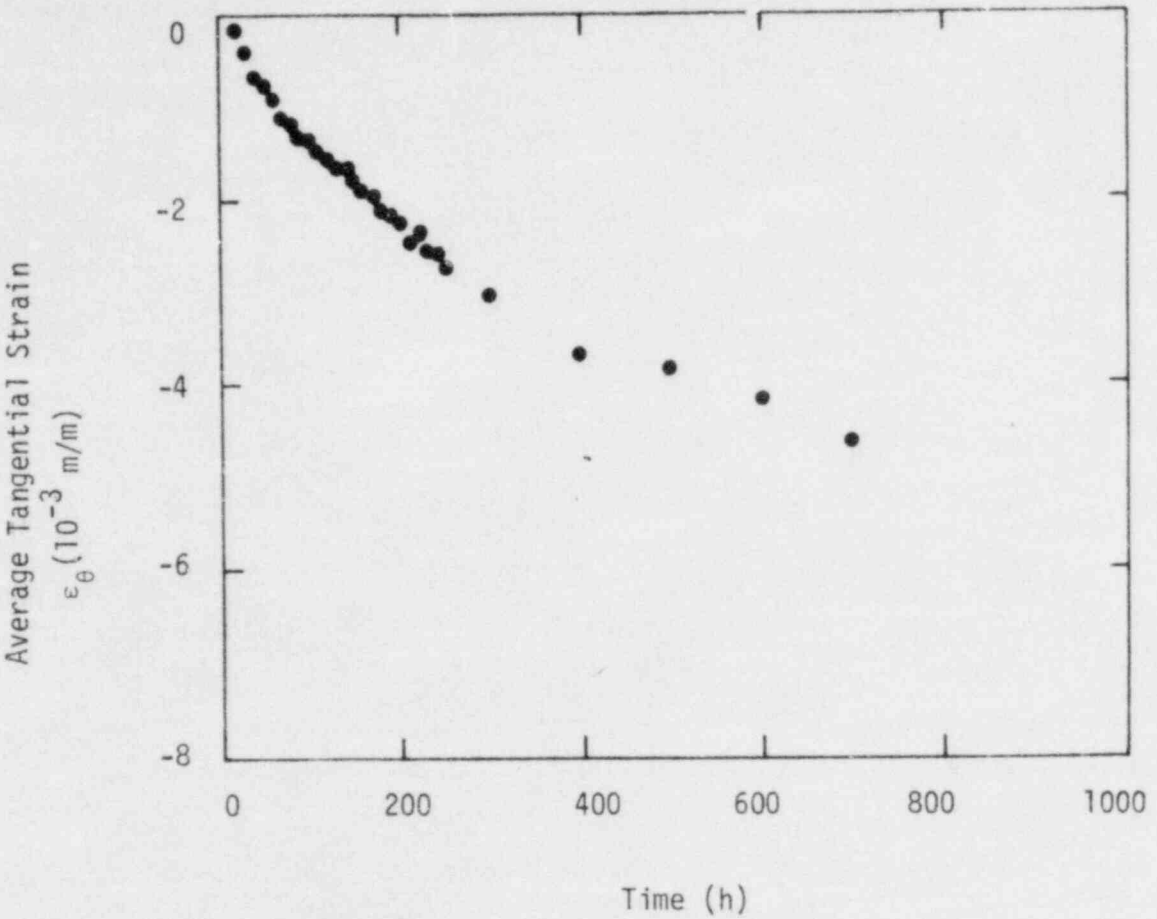

Fig. B-7.4 Average tangential strain as a function of time at 14.48 MPa differential pressure.

times and comparing the predicted strains to strain-time pairs not used in determining the constants A and B. Neither equation passed this test. Equation (B-7.11) consistently had too much curvature[a] and Equation (B-7.12) had too little curvature.

The equation finally adopted for short-time out-of-pile tests was

$$\varepsilon_\theta = A\,[1 - \exp(-Bt)] \qquad \text{(B-7.18)}$$

where

ε_θ = average tangential strain (m/m)

t = time (s)

A,B = functions of stress and temperature

For the 14.85 MPa test,

$$A = -5.32 \times 10^{-3} \text{ and } B = 7.64 \times 10^{-7}\text{s}.$$

For the 15.86 MPa tests,

$$A = -6.32 \times 10^{-3} \text{ and } B = 9.17 \times 10^{-7}\text{ s}.$$

The values of A and B for each stress were determined with a two-step process:

(1) A value of B was guessed and one strain-time pair (ε_0, t_0) was selected as a reference. Other strain-time pairs (ε_j, t_j), were then used to find an improved guess for B according to the relation

---

[a] $\left(\frac{d^2\varepsilon_\theta}{dt^2}\right)$ too large.

$$B_j = \ln\left[1 - \frac{\varepsilon_j \left[1 - \exp\left(-B_{guessed}\, t_o\right)\right]}{\varepsilon_o}\right] \qquad \text{(B-7.19)}$$

(2) Once a single value of B which worked for several strain-time pairs was determined, a least-squares-fit was carried out to determine A.

The two sets of values for A and B were used to estimate the effect of change in stress. A and B were assumed to be dependent on stress to some power, n, and n was calculated from A and B at the two stresses where they are known

$$n_A = \frac{\ln\left(\frac{A \text{ at } 15.86 \text{ MPa}}{A \text{ at } 14.48 \text{ MPa}}\right)}{\ln\left(\frac{15.86}{14.48}\right)} = 1.89 \qquad \text{(B-7.20a)}$$

$$n_B = \frac{\ln\left(\frac{B \text{ at } 15.86 \text{ MPa}}{B \text{ at } 14.48 \text{ MPa}}\right)}{\ln\left(\frac{15.86}{14.48}\right)} = 2.01 \qquad \text{(B-7.20b)}$$

In view of the limited number of tests, both values of n were assumed to be 2. This result implies a strain rate proportional to the fourth power of stress[a], a conclusion which agrees with one of the intermediate stress regions suggested by Dollins and Nichols mentioned in Section B-7.2.

The resultant expressions for the stress dependence of A and B near 125 MPa and at a temperature of 644 K are

$$A = (-5.32 \times 10^{-3}) \frac{\sigma^2}{(1.245 \times 10^8)^2} \qquad \text{(B-7.21)}$$

---

[a] The time derivative of Equation (B-7.18) is proportional to A times B.

$$B = (7.64 \times 10^{-7}) \frac{\sigma^2}{(1.245 \times 10^8)^2} \qquad \text{(B-7.22)}$$

where

σ = tangential component of stress.

The data from Hobson's in-reactor experiment were converted to average tangential strains with the same technique used for the out-of-reactor experiment. Figure B-7.5 displays the resultant average tangential strains as a function of time, along with the predicted out-of-reactor average strain from Equations (B-7.18), (B-7.21), and (B-7.22). The temperature during the in-reactor experiment was approximately the same as the temperature of Hobson's out-of-reactor experiments, but the pressure varied from 13 to 13.5 MPa so the tangential stress (-116 MPa) was smaller in magnitude than the stresses of the out-of-pile experiments.

Interpretation of the in-reactor data is complicated by the absence of data for the first eighty hours, by the reactor shutdown from 540 hours to 610 hours, and by the apparent positive average tangential strains from 80 to 200 hours. Hobson[B-7.24] has discussed the apparent positive average strains during the early part of the experiment and suggests that the positive readings come from the effects of a reactor scram at 50 hours on the experiment electronics.

The in-reactor strains shown in Figure B-7.5 are consistent with a simple relation between the out-of-reactor strains and the in-reactor strains (for fast neutron flux $\approx 5.4 \times 10^{17}$ neutrons/(m^2s)). The dashed line of the figure is the strain predicted by assuming that the initial out-of-reactor strain rate, AB, is maintained throughout the in-reactor experiment. The strains are described to within the experimental uncertainty by this line.

If this simple relation between initial out-of-reactor creep rates and in-reactor creep is confirmed by subsequent experiments with compressive stress, the implications for model development are significant. The result implies that irradiation-induced creep for compressive stress

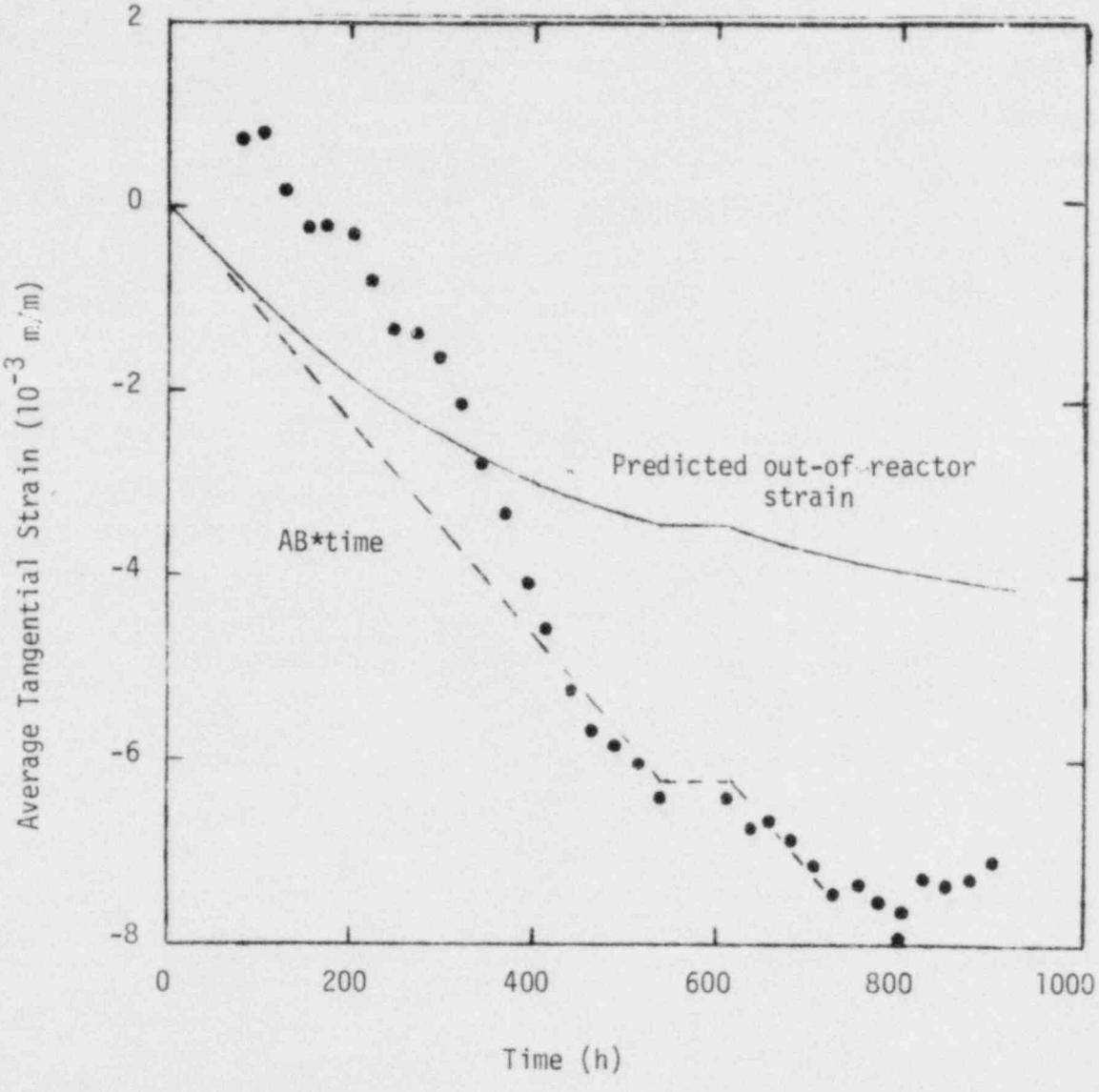

Fig. B-7.5 Average tangential strain as a function of time in Hobson's first in-pile experiment[B-7.24].

is not an independent additional creep (as virtually all the models based on tensile deformation data have assumed) but simply the result of destruction of some effect associated with prior creep strain which impedes further creep strain. In the absence of any data other than those from Hobson's experiments, the assumption must be made that either (a) the in-reactor creep rate is related to the initial out-of-reactor creep rate for compressive stress at temperatures near 644 K, or (b) that the fast neutron flux, stress magnitude and temperature are coincidentally at values which make the independent irradiation induced creep rate equal to the initial out-of-reactor creep rate. The author has selected assumption (a) and has proceeded to develop a model for cladding creep-down which is consistent with this assumption.

In order to be consistent with the assumption that some effect associated with prior creep strain impedes further creep strain, the independent variable in Equation (B-7.18) was changed from time to prior strain. The equation was differentiated with respect to time and the differentiated expression was used with Equation (B-7.18) to eliminate time. The resultant expression is

$$\dot{\varepsilon}_\theta = B\,[A - \varepsilon_\theta] \qquad \text{(B-7.23)}$$

where $\dot{\varepsilon}_\theta$ is the time derivative of the tangential strain (s^{-1}).

If fast neutron flux destroys some effect associated with prior creep strain, the appropriate modification of Equation (B-7.23) to describe in-reactor creep will reduce or eliminate the term $-B\varepsilon_\theta$ when a fast neutron flux is present. This was accomplished by adapting the idea of an auto-correlation function from statistical mechanics[B-7.27]. The total strain in Equation (B-7.23) is replaced by the integral of the strain increment at a prior time, t', times a correlation function which approximates the rate of destruction of the effect of prior strain on the current strain rate. In the absence of detailed information, the correlation function is represented by an exponential. The resultant generalization of Equation (B-7.23) is

$$\dot{\varepsilon}_\theta = B\left[A - \int_o^t \exp\left(-[t-t']\left[\frac{\phi}{\Psi} + \frac{1}{\tau}\right]\right) d\varepsilon(t')\right] \qquad \text{(B-7.24)}$$

where

ϕ = fast neutron flux (neutrons/(m^2s))

Ψ = the correlation fluence (neutrons/m^2)

τ = the zero flux correlation time (s)

and the other symbols have been previously defined.

The new parameters introduced in Equation (B-7.24) can be given a physical interpretation without defining a detailed mechanistic model. The correlation fluence, Ψ, is the amount of radiation damage required to destroy most of the effect of prior strain on current strain rate and the zero flux correlation time, τ, is the time at temperature required to anneal most of the effect of prior strain in zero flux. Since Equation (B-7.1) is an alternate form of Equation (B-7.24), the same interpretation can be applied to Equation (B-7.1).

The equations used in the CCSTRN subcode, Equations (B-7.6) and (B-7.7), are approximations derived from Equation (B-7.1). Equation (B-7.6) is obtained from Equation (B-7.1) by assuming

$$t\left[\frac{\phi}{\Psi} + \frac{1}{\tau}\right] << 1 \qquad \text{(B-7.25)}$$

and integrating Equation (B-7.1) from an initial to a final time, t. Equation (B-7.7) uses the steady state approximation to Equation (B-7.1), derived by setting the time derivative of Equation (B-7.1) equal to zero and solving for the steady-state creep rate. If the creep rate at the given final time of a time step interval is greater than or equal to the steady-state creep rate, Equation (B-7.6) is employed for the entire time interval. If the creep rate at the given final time of a time step interval is less than the steady state creep rate, the time to steady state is calculated with Equation (B-7.8) and Equation (B-7.7)

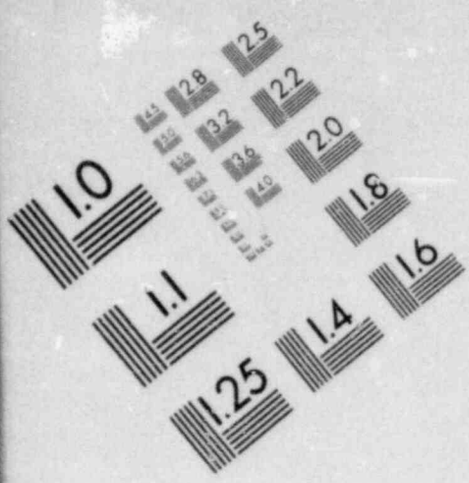

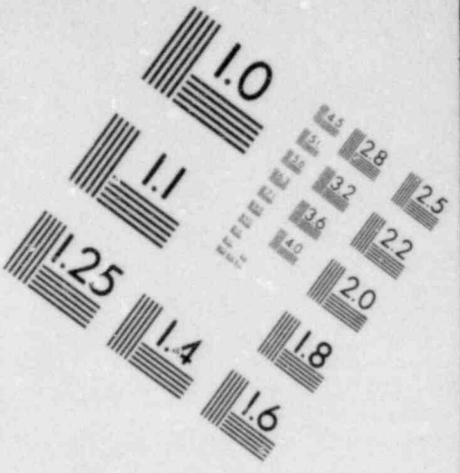

IMAGE EVALUATION
TEST TARGET (MT-3)

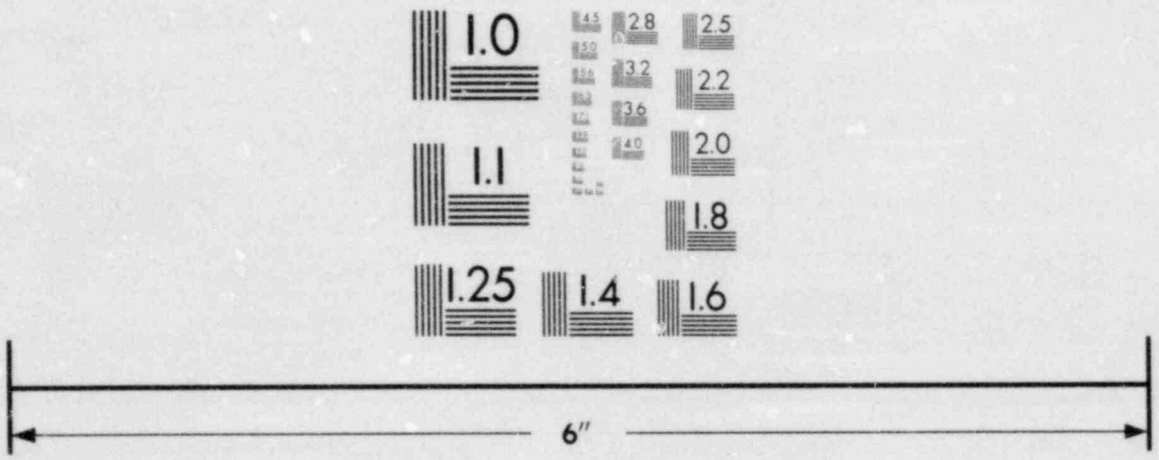

MICROCOPY RESOLUTION TEST CHART

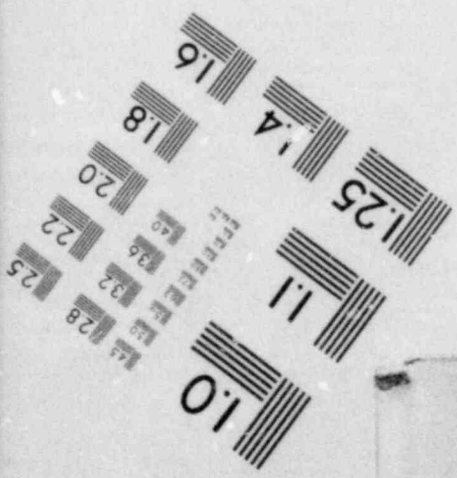

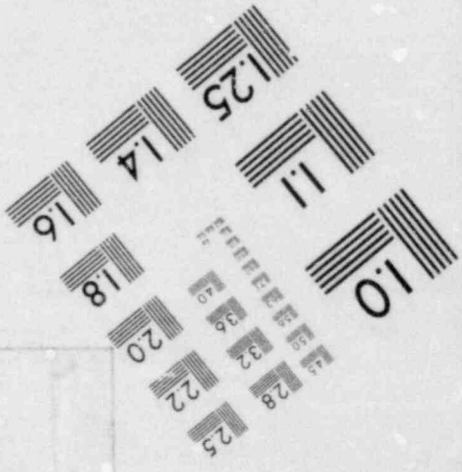

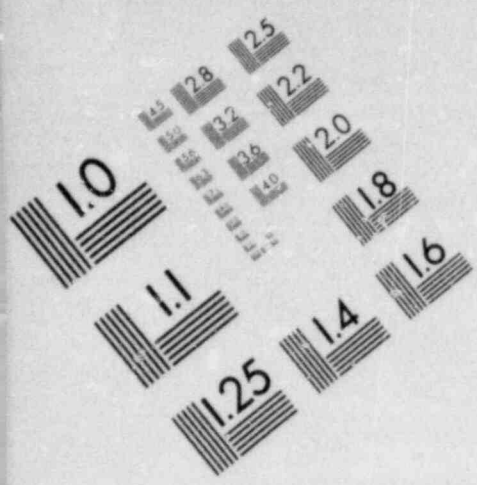

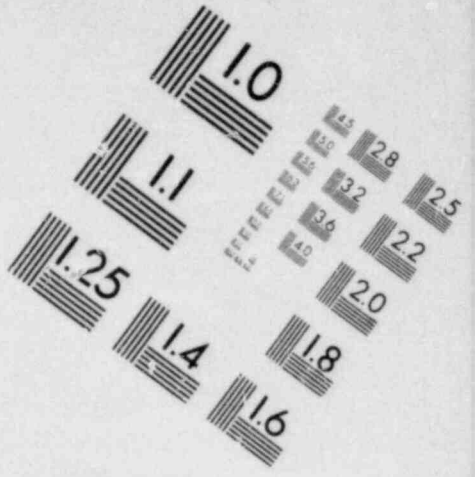

IMAGE EVALUATION
TEST TARGET (MT-3)

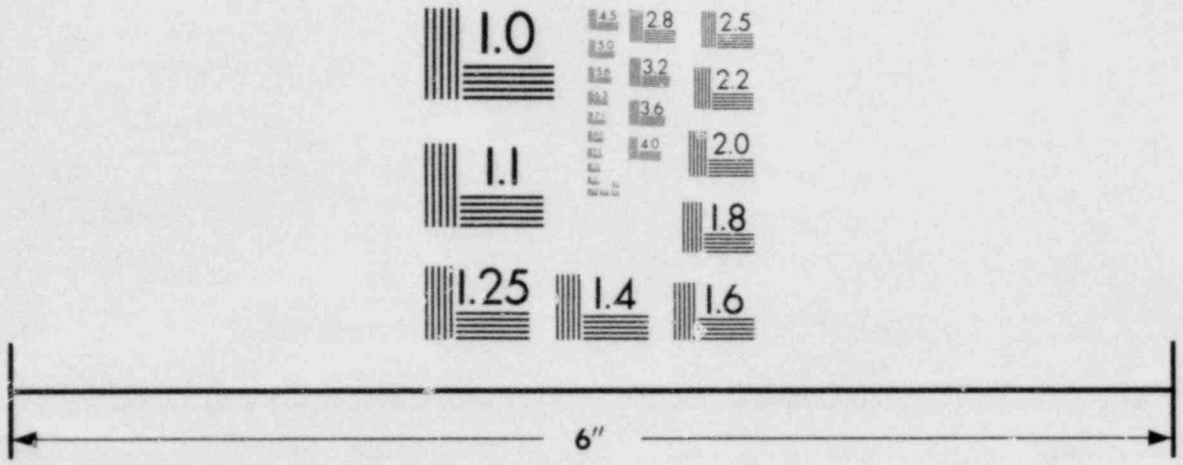

MICROCOPY RESOLUTION TEST CHART

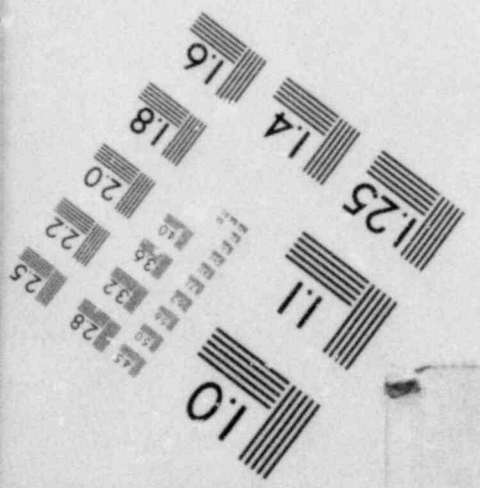

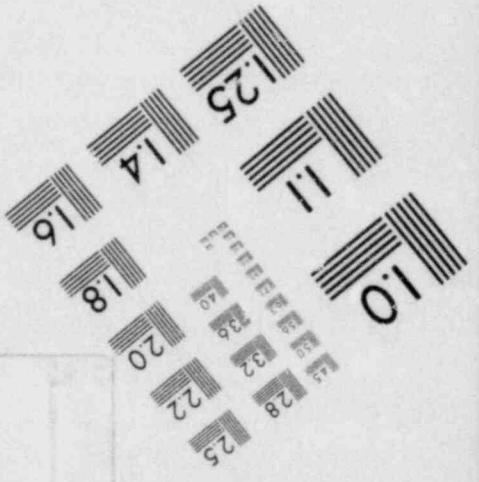

is used to calculate the final strain from the assumption that the creep rate after the time interval given by Equation (B-7.8) has passed. The time interval to steady state is found by solving the time derivative of Equation (B-7.6) for the time when the creep rate is equal to the steady state creep rate.

Equations (B-7.6) and (B-7.7) contain a term, $\varepsilon_{boundary}$, which is the initial creep strain for any time step in which the temperature and stress are the same as the previous time step. For time steps in which the temperature, stress, or fast neutron flux has changed, Equation (B-7.1) implies that the creep rate should respond immediately to changes in the product AB (a function of stress and temperature) but the response of the creep rate to changes in the factor $\frac{\phi}{\Psi} + \frac{1}{\tau}$ (a function of flux and temperature) should be more gradual. A boundary condition is therefore required to make the initial creep rate of Equation (B-7.6) equal to the creep rate at the end of the prior step. The appropriate condition is

$$\varepsilon_{boundary} = AP \exp(-BP\ \Delta tp) + \varepsilon P_{boundary}\ [1-\exp(-BP\Delta tp)]$$

for prior steps not in steady state

$$= \frac{AP\ BP}{\frac{\phi P}{\Psi P} + \frac{1}{\tau P} + BP} \qquad \text{(B-7.26)}$$

for prior steps in steady state

where AP, BP, ΔtP, $\varepsilon P_{boundary}$, ϕP, ΨP and τP are the values of A, B, Δt, $\varepsilon_{boundary}$, ϕ, Ψ, and τ during the previous time step.

Values for the parameters A and B at 644 K and stresses near 125 MPa have been determined from Hobson's out-of-reactor data. These data can also be used in conjunction with the modeling ideas just developed to find a minimum value for the zero flux correlation time, τ, at 644 K. The strains shown in Figure B-7.3 show that a steady state creep rate (i.e., a straight line plot for strain versus time) did not occur prior

to 600 hours in either of the out-of-reactor experiments represented in the figure. Equation (B-7.8) with ϕ=0 and Δt_{ss} at least as large as 600 hours implies a τ of at least 6.8×10^6s. This value was adopted as an interim estimate for τ at 644 K since the strains calculated from test 269-27 (the test which simulated an axial gap in the fuel pellets) are consistent with steady state creep after 600 hours.

The temperature dependent factors in Equations (B-7.3), (B-7.4) and (B-7.5) are interim estimates because they are based on the temperature dependence of tensile creep data. The data from Fidleris' tests R-6 and Rx-14[B-7.11] were selected to estimate the temperature dependence of B, τ, and Ψ because these tests were carried out at a stress magnitude which closely approximates the magnitude of the stress in Hobson's experiments.

Figure B-7.6 illustrates the steady state creep rates reported by Fidleris for a stress of 138 MPa at several temperatures. The in-reactor data are at fast neutron fluxes of 6.8×10^{16} or 6.0×10^{16} neutrons/(m^2s). The range of steady state creep rates predicted by the model for creep down at 644 K is also represented and a solid square is used to represent the steady state creep rate seen in Hobson's experiment at a fast neutron flux of 5.4×10^{17} neutrons/(m^2s). The slope of the tensile stress data at temperatures above 614 K ($\frac{1}{T}$ less than 1.626×10^{-3}) corresponds to a temperature dependent factor of the form $\exp\left(\frac{-25,100}{T}\right)$ and the in-reactor data below 615 K correspond to a temperature dependent factor of the form $\exp\left(\frac{-10,400}{T}\right)$. The temperature dependent factors in Equations (B-7.3), (B-7.4) and (B-7,5) are the most convenient way of forcing the steady state creep rate implied by Equation (B-7.7) to correspond to the temperature dependence shown by the Fidleris equation.

The constants 2.9×10^6 and 6.967795×10^{16} in Equation (B-7.4) are the result of a least squares fit to the steady state creep rate data

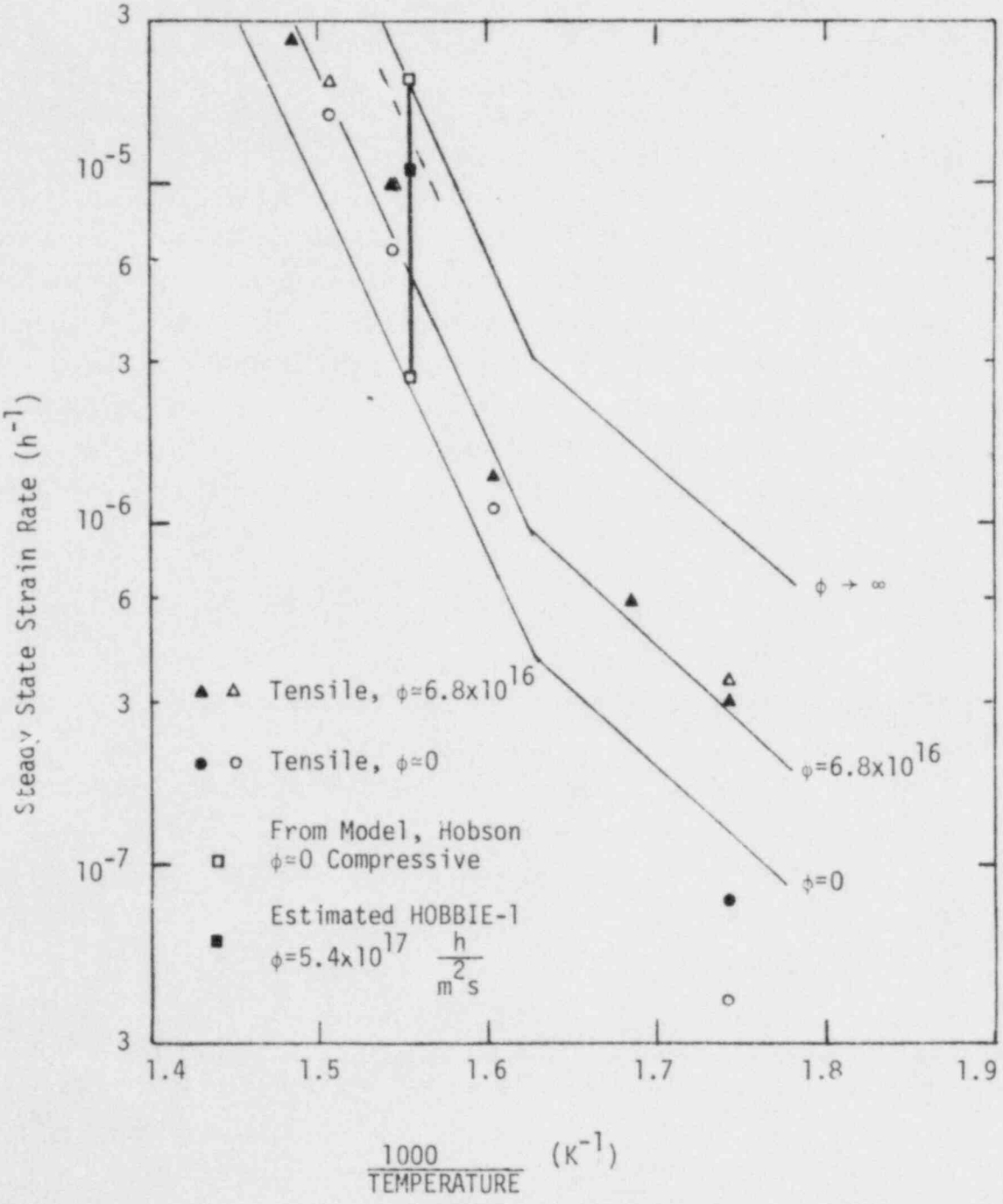

Fig. B-7.6 Steady state creep rates reported by Fidleris[B-7] for tests R-6 and Rx-14 and model predictions for steady state creepdown rates derived from these data.

of Fidleris. As expected from the discussion of the previous section, the resultant prediction of the steady-state creep rate for Hobsons in-reactor creep rate at 5.4 x 10^{17} neutrons/(m^2s) with a compressive stress is slightly too high. The predicted rate, s^{-1}, is shown in Figure B-7.6 by the dashed line.

7.4 Uncertainty of the Model

The lack of an extensive data base for creep under compressive stress makes the assignment of uncertainty limits very tentative. The data of Stehle which are illustrated in Figure B-7.1 of Section 7.2 are the only other compressive stress data available. These data show creep strains of about half the magnitude of the model predicted strains. Since these are the only appropriate data not used in developing the model, they were used to estimate fractional error of -0.6 and +0.3 in strain at 644 K and -130 MPa stress. The remaining terms of the uncertainty estimate for the strain predicted by CCSTRN, Equation (B-7.9), are simply engineering judgements which estimate 100% error when the stress differs from -130 MPa by more than 65 MPa or the temperature differs from 644 K by more than 60 K.

Equation (B-7.10), the expression for the uncertainty of the stress calculated by the CCSTRS subroutine, was derived from Equation (B-7.9) and the observation that the predicted strain is usually proportional to the fourth power of stress. The resultant uncertainty in stress expressed as a fraction of stress is one-fourth the fractional uncertainty in strain.

7.5 Cladding Creepdown Subcodes (CCSTRN and CCSTRS) Listings

Listings of the FORTRAN subcodes CCSTRN for creep strain as a function of stress and CCSTRS for stress as a function of creep strain increment are given in Tables B-7.III and B-7.IV. Uncertainty estimates are computed within the subcodes, but are not returned.

TABLE B-7.III

LISTING OF THE CCSTRN SUBCODE

```
      SUBROUTINE CCSTRN(CTEMP,DELT,CFLUX,CHSTRS,CSTNB,CCSTNI,
     # CSTNBN,CCSTNF)
C
C     CCSTRN CALCULATES THE TANGENTIAL COMPONENT OF CLADDING
C     CREEP STRAIN AT THE END OF A TIME STEP WITH CONSTANT
C     CLADDING TEMPERATURE, FLUX, AND STRESS.
C
C     CCSTNF = OUTPUT TANGENTIAL COMPONENT OF CLADDING CREEP
C              STRAIN AT THE END OF THE TIME STEP (M/M)
C     CSTNBN = OUTPUT BOUNDARY CONDITION PARAMETER USED TO
C              SPECIFY INITIAL SLOPE OF NEXT TIME STEP (UNITLESS)
C     USTNU  = ESTIMATED UNCERTAINTY OF STRAIN INCREMENT --
C              UPPER BOUND ON STRAIN INCREMENT MAGNITUDE (UNITLESS).
C              CALCULATED BUT NOT RETURNED.
C     USTNL  = ESTIMATED UNCERTAINTY OF STRAIN INCREMENT --
C              LOWER BOUND ON STRAIN INCREMENT MAGNITUDE (UNITLESS).
C              CALCULATED BUT NOT RETURNED.
C
C
C     CTEMP  = INPUT CLADDING TEMPERATURE (K)
C     DELT   = INPUT TIME STEP SIZE (S)
C     CFLUX  = INPUT FAST NEUTRON FLUX (NEUTRONS/((M**2)*S))
C     CHSTRS = INPUT TANGENTIAL COMPONENT OF CLADDING STRESS (PA)
C     CSTNB  = INPUT BOUNDARY CONDITION PARAMETER USED TO
C              SPECIFY INITIAL SLOPE OF CURRENT TIME STEP
C              (UNITLESS).
C              THIS PARAMETER IS ZERO FOR THE FIRST TIME STEP
C              AND IS TAKEN FROM OUTPUT FOR SUBSEQUENT STEPS.
C     CCSTNI = INPUT TANGENTIAL COMPONENT OF CLADDING CREEP
C              STRAIN AT THE START OF THE TIME STEP (M/M)
C
C     THE EQUATIONS USED IN THIS SUBROUTINE ARE BASED ON DATA FROM
C     (1) D. O. HOBSON, CREEPDOWN OF ZIRCALOY FUEL CLADDING
C         INITIAL TESTS, ORNL/NUREG/TM-181 (APRIL 1978).
C      (2) D. O. HOBSON, PRELIMINARY ANALYSIS OF SURFACE DISPLACEMENT
C         RESULTS IN THE CREEPDOWN IRRADIATION EXPERIMENT HOBBIE-1,
C         ORNL/NUREG/TM-310 (JUNE 1979).
C     (3) V. FIDLERIS, UNIAXIAL IN-REACTOR CREEP OF ZIRCONIUM
C         ALLOYS, JOURNAL OF NUCLEAR MATERIALS 26 (1968).
C         PP. 51-76.
C     (4) H. STEHLE ET AL., MECHANICAL PROPERTIES OF ANISOTROPY
C         AND MICROSTRUCTURE OF ZIRCALOY CANNING TUBES,
C         ZIRCONIUM IN THE NUCLEAR INDUSTRY, ASTM STP 663
C         (1977) PP. 486-507.
C
C     THE SUBCODE CABTP IS USED IN THIS SUBROUTINE
C
C     CCSTRN WAS CODED BY D. L. HAGRMAN MAY 1980
C
      CALL CABTP(CTEMP,CHSTRS,A,B,TAU,PSI)
C
C     CHECK FOR PRE OR POST STEADY STATE CREEP
      RCT = CFLUX/PSI + 1.0/TAU
C
      Z = A/((1.0 + B/RCT) * (A - CSTNB))
      DTSS = 0.0
      IF(Z .LE. 0. .OR. Z .GE. 1. ) GO TO 10
      DTSS = -( ALOG(Z)/B)
```

TABLE B-7.III (Contd.)

```
C
C     BRANCH FOR PRE OR POST STEADY STATE CREEP
      IF(DELT .GE. DTSS) GO TO 10
      CCSTNF =  (A - CSTNB) * (1. -  EXP(-B*DELT)) + CCSTNI
      CSTNBN = -( EXP(-B*DELT))*( A - CSTNB ) + A
      GO TO 20
   10 CCSTNF = (A - CSTNB) * (1. - EXP(-B*DTSS)) + CCSTNI
     #   + ( B * A / ( 1. + B/RCT) ) * ( DELT - DTSS)
      CSTNBN = A * B / RCT
C
C     ESTIMATE UNCERTAINTY IN STRAIN INCREMENT
   20 UCTR = 2. * ABS( (CHSTRS + 1.3E+08)/1.3E+08)
     #      + 5. * ABS( (CTEMP - 644.)/644.)
      USTNU = (1. + 0.3 * ( 1. + UCTR)) * (CCSTNF - CCSTNI)
      USTNL = (0.4 / ( 1. + UCTR )) * (CCSTNF - CCSTNI)
C
      RETURN
      END
```

```
      SUBROUTINE CABTP(CTEMP,CHSTRS,A,B,TAU,PSI)
C
CC    CABTP CALCULATES PARAMETERS FOR THE CLADDING CREEP DOWN
CC      SUBROUTINE CCSTRN
CC
CC    A       = OUTPUT ULTIMATE STRAIN FOR INFINITE CORRELATION
CC              (UNITLESS).
CC    B       = OUTPUT RATE CONSTANT (S**(-1))
CC    TAU     = OUTPUT ZERO FLUX CORRELATION TIME (S).
CC    PSI     = OUTPUT CORRELATION FLUENCE (NEUTRONS/((M**2)*S))
CC
CC    CTEMP   = INPUT CLADDING TEMPERATURE (K)
CC    CHSTRS  = INPUT TANGENTIAL COMPONENT OF CLADDING STRESS (PA)
C
      T = CTEMP
      IF(CTEMP .GT. 750.) T = 750.
      IF(CTEMP .LT. 450.) T = 450.
      S =  ABS(CHSTRS)
C
CC    APPROXIMATE STRESS EXPONENT BY COMPARISON TO STRENGTH
C     COEFFICIENT APPROXIMATION
      AK = 1.5E+09 -  1.5E+06 * T
C
      A = 3.83E-19  * (S**3) /CHSTRS
      IF(S .LT. (0.20 * AK)) A = A * ((0.20 * AK / S )**1.5)
      IF(S .GT. (0.75 * AK)) A = A * ((S/(0.75 * AK))**23)
C
      IF(T .LT. 615.) GO TO 10
      B = 4.69E-06 * (S**2) *  EXP(-2.51E+04/T)
      TAU = 8.6E-11 *  EXP(2.51E+04/T)
      PSI = 2.9E+06  *  EXP(2.51E+04/T)
      GO TO 20
   10 B = 1.9519804E-16 * (S**2) *  EXP(-1.04E+04/T)
      TAU = 2.0663116 *  EXP(1.04E+04/T)
      PSI = 6.967795E+16 *  EXP(1.04E+04/T)
   20 IF(S .LT. (0.20 * AK)) B = B * ((0.20 * AK / S )**1.5)
      IF(S .GT. (0.75 * AK)) B = B * ((S/(0.75 * AK))**23)
      RETURN
      END
```

TABLE B-7.IV

LISTING OF THE CCSTRS SUBCODE

```
      SUBROUTINE CCSTRS(CTEMP,DELT,CFLUX,CSTNB,CCSTNI,CCSTNF,
     # CSTNBN,CHSTRS)
C     CCSTRS CALCULATED THE TANGENTIAL COMPONENT OF CLADDING
C     CREEP STRESS DURING A TIME STEP WITH CONDTANT
C     CLADDING TEMPERATURE, FLUX, AND STRESS.
C
C     CHSTRS = OUTPUT TANGENTIAL COMPONENT OF CLADDING STRESS (PA)
C     CSTNBN = OUTPUT BOUNDARY CONDITION PARAMETER USED TO
C              SPECIFY INITIAL SLOPE OF NEXT TIME STEP (UNITLESS)
C     USTRU  = ESTIMATED UNCERTAINTY OF THE STRESS MAGNITUDE --
C              UPPER BOUND ON STRESS MAGNITUDE (PA)
C     USTRL  = ESTIMATED UNCERTAINTY OF THE STRESS MAGNITUDE --
C              LOWER BOUND ON STRESS MAGNITUDE (PA)
C     CTEMP  = INPUT CLADDING TEMPERATURE (K)
C     DELT   = INPUT TIME STEP SIZE (S)
C     CFLUX  = INPUT FAST NEUTRON FLUX (NEUTRONS/((M**2)*S))
C     CSTNB  = INPUT BOUNDARY CONDITION PARAMETER USED TO
C              SPECIFY INITIAL SLOPE OF CURRENT TIME STEP
C              (UNITLESS).
C              THIS PARAMETER IS ZERO FOR THE FIRST TIME STEP
C              AND IS TAKEN FROM OUTPUT FOR SUBSEQUENT STEPS.
C     CCSTNI = INPUT TANGENTIAL COMPONENT OF CLADDING CREEP
C              STRAIN AT THE START OF THE TIME STEP (M/M)
C     CCSTNF = INPUT TANGENTIAL COMPONENT OF CLADDING CREEP
C              STRAIN AT THE END OF THE TIME STEP (M/M)
C
C     THE EQUATIONS USED IN THIS SUBROUTINE ARE BASED ON DATA FROM
C     (1) D. O. HOBSON, CREEPDOWN OF ZIRCALOY FUEL CLADDING
C         INITIAL TESTS, ORNL/NUREG/TM-181 (APRIL 1978).
C      (2) D. O. HOBSON, PRELIMINARY ANALYSIS OF SURFACE DISPLACEMENT
C         RESULTS IN THE CREEPDOWN IRRADIATION EXPERIMENT HOBBIE-1,
C         ORNL/NUREG/TM-310 (JUNE 1979).
C     (3) V. FIDLERIS, UNIAXIAL IN-REACTOR CREEP OF ZIRCONIUM
C         ALLOYS, JOURNAL OF NUCLEAR MATERIALS 26 (1968).
C         PP. 51-76.
C     (4) H. STEHLE ET AL., MECHANICAL PROPERTIES OF ANISOTROPY
C         AND MICROSTRUCTURE OF ZIRCALOY CANNING TUBES,
C         ZIRCONIUM IN THE NUCLEAR INDUSTRY, ASTM STP 663
C         (1977) PP. 486-507.
C
C     THE SUBCODE CTP IS USED IN THIS SUBROUTINE
C
C     CCSTRS WAS CODED BY D. L. HAGRMAN JUNE 1980
C
C     X = AC * (ABS(STRESS) ** 0.5  2.0  OR  25.)
C     Y = X/AC
C
      CALL CTP(CTEMP,BC,TAU,PSI,AK)
      AC = 3.83E-19
      RCT = CFLUX/PSI + 1.0/TAU
      DELSTN = CCSTNF - CCSTNI
C
```

TABLE B-7.IV (Contd.)

```
C       BRANCH FOR POSITIVE OR NEGATIVE STRAIN INCREMENT
        IF(DELSTN .EQ. 0.) GO TO 800
        IF(DELSTN .GT. 0.) GO TO 300
C
C       BRANCH FOR SUBCASES OF NEGATIVE STRAIN INCREMENT
        IF((CSTNB + DELSTN) .GT. 0.) GO TO 110
C
C       SUBCASE ONE  CSTNB + DELSTN IS NEGATIVE
        ARG = BC * DELT * (CSTNB + DELSTN) / AC
        IF(ARG .LT. -030.) GO TO 260
        XL = - ( CSTNB  + DELSTN )
        CXP =  EXP(ARG)
        DELTA = AC * DELSTN /(-AC*(1. - CXP) + DELSTN * BC * DELT * CXP)
        GO TO 210
C
C       SUBCASE TWO  CSTNB + DELSTN IS POSITIVE
  110 XL = 0.
        DELTA = -AC * DELSTN / (CSTNB  * BC * DELT)
C
  210 N = 0
        M = 0
  215 XH = XL + DELTA
        STN      =(-XH- CSTNB) * (1. -  EXP(-BC * DELT * XH/AC))
        IF(STN .GE. DELSTN) GO TO 220
        DELTA = DELTA / 5.
        M = M + 1
        IF(M .LT. 5) GO TO 215
  220 XH = XL + DELTA
        STN      =(-XH- CSTNB) * (1. -  EXP(-BC * DELT * XH/AC))
        IF(STN .LT. DELSTN) GO TO 230
        DELTA = DELTA * 2.
        N = N + 1
        IF(N .LT. 5) GO TO 220
  230 CONTINUE
        N = 0
        XM = (XL + XH) * 0.5
        STNM     =(-XM- CSTNB) * (1. -  EXP(-BC * DELT * XM/AC))
  240 IF(STNM .LT. DELSTN) XH = XM
        IF(STNM .GE. DELSTN) XL = XM
        XM = (XL + XH) * 0.5
        STNM     =(-XM- CSTNB) * (1. -  EXP(-BC * DELT * XM/AC))
        FE =  ABS(STNM/DELSTN - 1.0)
        IF(FE .LT. 0.01) GO TO 250
        N = N + 1
        IF(N .LT. 11) GO TO 240
  250 A = - XM
        GO TO 500
  260 XM = -DELSTN - CSTNB
        A = -XM
        GO TO 500
C
C       POSITIVE STRAIN INCREMENT
C
C       BRANCH FOR SUBCASES OF POSITIVE STRAIN INCREMENT
  300 IF((CSTNB + DELSTN) .LT. 0.) GO TO 310
C
C       SUBCASE ONE  CSTNB + DELSTN IS POSITIVE
        ARG =-BC * DELT * (CSTNB + DELSTN) / AC
        IF(ARG .LT. -030.) GO TO 460
        XL = CSTNB + DELSTN
        CXP =  EXP(ARG)
        DELTA = AC * DELSTN / (AC*(1. - CXP) + DELSTN * BC * DELT * CXP)
        GO TO 410
C
```

TABLE B-7.IV (Contd.)

```
C     SUBCASE TWO  CSTNB + DELSTN IS NEGATIVE
  310 XL = 0.
      DELTA = -AC * DELSTN / (CSTNB  * BC * DELT)
  410 N = 0
      M = 0
  415 XH = XL + DELTA
      STN     = (XH- CSTNB) * (1. -  EXP(-BC * DELT * XH/AC))
      IF(STN .LE. DELSTN) GO TO 420
      DELTA = DELTA / 5.
      M = M + 1
      IF(M .LT. 5) GO TO 415
  420 XH = XL + DELTA
      STN     = (XH- CSTNB) * (1. -  EXP(-BC * DELT * XH/AC))
      IF(STN .GT. DELSTN) GO TO 430
      DELTA = DELTA * 2.
      N = N + 1
      IF(N .LT. 5) GO TO 420
  430 CONTINUE
      N = 0
      XM = (XL + XH) * 0.5
      STNM    = (XM- CSTNB) * (1. -  EXP(-BC * DELT * XM/AC))
  440 IF(STNM .LT. DELSTN) XL = XM
      IF(STNM .GE. DELSTN) XH = XM
      XM = (XL + XH) * 0.5
      STNM    = (XM- CSTNB) * (1. -  EXP(-BC * DELT * XM/AC))
      FE = ABS(STNM/DELSTN - 1.0)
      IF(FE .LT. 0.01) GO TO 450
      N = N + 1
      IF(N .LT. 11) GO TO 440
  450 A = XM
      GO TO 500
  460 XM = DELSTN + CSTNB
      A = XM
C
CC    BRANCH FOR PRE OR POST STEADY STATE
C
  500 B = BC * XM/ AC
      Z = A / ((A - CSTNB) * (1. + B/RCT))
      W = 1.
      IF(DELSTN .LT. 0.) W = -1.
      IF(Z .GE. 1.) GO TO 510
      DTSS = -(  ALOG(Z))/B
      Y = XM/ AC
      ARG = -B * DELT
      IF(ARG .GE. -030.) CSTNBN = -(  EXP(ARG)) * (A - CSTNB) + A
      IF(ARG .LT. -030.) CSTNBN = A
      IF(DELT .LE. DTSS) GO TO 700
C
CC    TREAT THE CASE WHERE THE WHOLE STEP IS STEADY STATE AND
CC    FIND UPPER LIMITS OF ABS(STRESS) FOR TRANSITION CASE
C     STRESS FOR PURE STEADY STATE
  510 EDAV =  ABS(DELSTN)/DELT
      Y = (EDAV/(2. * RCT * AC)) * (1.0 + (1.0 + 4. * AC * RCT * RCT /
     # (BC * EDAV) )**0.5)
C     CHECK TO SEE IF PURE STEADY STATE IS CONSISTENT
      Z = W * Y * AC /((W * Y * AC - CSTNB)*(1. + BC*Y /RCT))
      CSTNBN =-AC * BC * (Y**2) / RCT
      IF(Z .LE. 0. .OR. Z .GE. 1.) GO TO 700
C
```

TABLE B-7.IV (Contd.)

```
C     TREAT THE CASE WHERE ONLY PART OF THE STEP IS STEADY STATE
C     XH IS UPPER LIMIT ON ABS STRESS.  PURE PRIMARY CASE IS THIS LIMIT
      XH = XM
C     XLL IS LOWER LIMIT ON ABS STRESS. PURE SS CASE SLOPE IS THIS LIMIT
      XLL = (W * CSTNB + (CSTNB**2 + 4.*((AC*Y)**2)/(1.+(BC*Y/RCT)))
     # **0.5)/2.
      DELTA = (XH - XLL)/10.
      IF(DELTA .LE. 0.) DELTA = XH/10.
      XL = XH
      N = 0
  610 XL = XL - DELTA
      BL = BC * XL / AC
      ZL = W * XL /((W* XL - CSTNB) * (1. + BL /RCT))
      DTSS = - (  ALOG(ZL)/BL)
      STNL = -CSTNB + BL * W * XL * ((1./RCT; + DELT - DTSS)
     # /(1. + (BL/RCT))
      IF((W * STNL) .LT. (W * DELSTN)) GO TO 620
      XH = XL
      N = N + 1
      IF(N .LT. 9) GO TO 610
      XL = XLL
  620 N = 0
  630 XM = (XL + XH) * 0.5
      BM = BC * XM / AC
      ZM = W * XM /((W * XM - CSTNB) * (1. + BM / RCT) )
      DTSS = -(  ALOG(ZM) / BM )
      STNL = -CSTNB + BM * W * XM * ((1./RCT) + DELT - DTSS)
     # /(1. + (BM/RCT))
      FE = ABS((STNL/DELSTN) - 1.0)
      IF(FE .LT. 0.01) GO TO 640
      IF((W * STNL) .LT. (W * DELSTN)) XL = XM
      IF((W * STNL) .GE. (W * DELSTN)) XH = XM
      N = N + 1
      IF(N .LT. 15) GO TO 630
  640 Y = XM/AC
      CSTNBN = W * XM * BM /RCT
C
C
  700 ALIMH = (0.75 * AK)**2
      ALIML = (0.20*AK)**2
      CHSTRS = W * (Y**0.5)
      IF(Y .GT. ALIMH) CHSTRS = W*(Y**0.04) * ((0.75*AK)**0.92)
      IF(Y .LT. ALIML) CHSTRS = W * (Y**2) / ((0.20*AK)**3)
      GO TO 810
  800 CHSTRS = 0.0
  810 CONTINUE
C
C     ESTIMATE UNCERTAINTY IN STRESS
      UCTR = 2. * ABS( (CHSTRS + 1.3E+08)/1.3E+08)
     #     + 5. * ABS( (CTEMP - 644.)/644.)
      USTRU = (1. + 0.075 * (1. + UCTR)) * CHSTRS
      USTRL = (0.85/(1. + UCTR)) * CHSTRS
C
      RETURN
      END
```

TABLE B-7.IV (Contd.)

```
      SUBROUTINE CTP(CTEMP,BC,TAU,PSI,AK)
C
C     CTP CALCULATES PARAMETERS FOR THE CLADDING CREEP DOWN
C       SUBROUTINE CCSTRS
C
C     BC      = OUTPUT STRESS COEFFICIENT OF RATE CONSTANT
C     TAU     = OUTPUT ZERO FLUX CORRELATION TIME (S).
C     PSI     = OUTPUT CORRELATION FLUENCE (NEUTRONS/((M**2)*S))
C
C     CTEMP   = INPUT CLADDING TEMPERATURE (K)
C
      T = CTEMP
      IF(CTEMP .GT. 750.) T = 750.
      IF(CTEMP .LT. 450.) T=450.
      AK =  1.5E+09 - 1.5E+06 * T
C
      IF(T .LT. 615.) GO TO 10
      BC = 4.69E-06 *  EXP(-2.51E+04/T)
      TAU = 8.6E-11 *  EXP(2.51E+04/T)
      PSI = 2.9E+06 *  EXP(2.51E+04/T)
      GO TO 20
   10 BC = 1.9519804E-16 *  EXP(-1.04E+04/T)
      TAU = 2.0663116 *  EXP(1.04E+04/T)
      PSI = 6.967795E+16 *  EXP(1.04E+04/T)
   20 CONTINUE
      RETURN
      END
```

7.6 References

B-7.1 C. C. Dollins and F. A. Nichols, "Mechanisms of Irradiation Creep in Zirconium-Base Alloys", Zirconium in Nuclear Applications, ASTM-STP-551, (1974) pp. 229-248.

B-7.2 G. R. Piercy, "Mechanisms for the In-Reactor Creep of Zirconium Alloys", Journal of Nuclear Materials, 25 (1968) pp 18-50.

B-7.3 C. R. MacEwen, "The Effect of Neutron Flux on Dislocation Climb", Journal of Nuclear Materials, 54 (1974) pp 85-96.

B-7.4 F. A. Nichols, "Point Defects and the Creep of Metals", Journal of Nuclear Materials, 69 and 70 (1978) pp 451-464.

B-7.5 F. A. Nichols, "On the SIPA Contribution to Irradiation Creep", Journal of Nuclear Materials, 84 (1979) pp 207-221.

B-7.6 D. O. Northwood, "Comments on In-Pile Dimensional Changes in Neutron Irradiated Zirconium Base Alloys", Journal of Nuclear Materials, 64 (1977) pp 316-319.

B-7.7 E. F. Ibrahim, "In-Reactor Creep of Zirconium Alloys by Thermal Spikes", Journal of Nuclear Materials, 58 (1975) pp 302-310.

B-7.8 P. A. Ross-Ross and C. E. L. Hunt, "The In-Reactor Creep of Cold-Worked Zircaloy-2 and Zirconium-2.5 wt Niobium Pressure Tubes", Journal of Nuclear Materials, 26 (1968) pp 2-17.

B-7.9 V. Fidleris, "Summary of Experimental Results on In-Reactor Creep and Irradiation Growth of Zirconium Alloys, Atomic Energy Review, 13 (1976) pp 51-80.

B-7.10 R. D. Warda, V. Fidleris, and E. Teghtsoonian, "Dynamic Strain Aging During Creep of α-Zr", Metallurgical Transactions 4 (1972/1973) pp 302-316.

B-7.11 V. Fidleris, "Uniaxial In-Reactor Creep of Zirconium Alloys", Journal of Nuclear Materials, 26 (1968) pp 51-76.

B-7.12 W. J. Duffin and F. A. Nichols, "The Effect of Irradiation on Diffusion-Controlled Creep Processes", Journal of Nuclear Materials, 45 (1972/1973) pp 302-316.

B-7.13 D. S. Wood, "Dose Dependence of Irradiation Creep of Zircaloy-2", Properties of Reactor Structural Alloys After Neutron or Particle Irradiation, ASTM-STP-570, (1975) pp 207-217.

B-7.14 D. S. Wood and B. Watkins, "A Creep Limit Approach to the Design of Zircaloy-2 Reactor Pressure Tubes at 275° C", Journal of Nuclear Materials, 41 (1971) pp 327-340.

B-7.15 E. Kohn, "In-Reactor Creep of Zr-2.5Nb Fuel Cladding", Zirconium in the Nuclear Industry, ASTM-STP-633 (1977) pp 402-417.

B-7.16 E. R. Gilbert, "In-Reactor Creep of Reactor Materials", Reactor Technology, 14 (Fall 1971) pp 258-285.

B-7.17 H. Stehle, et al., "Mechanical Properties of Anisotropy and Microstructure of Zircaloy Canning Tubes", Zirconium in the Nuclear Industry, ASTM-STP-663, American Society for Testing and Materials (December 1977) pp 486-507.

B-7.18 M. L. Picklesimer, "Deformation, Creep, and Fracture in Alpha-Zirconium Alloys", Electrochemical Technology, 4 (1966) pp 289-300.

B-7.19 G. E. Lucas and A. L. Bement, "Temperature Dependence of the Zircaloy-4 Strength Differential", Journal of Nuclear Materials 48 (1975) pp 163-170.

B-7.20 R. H. Chapman, Characterization of Zircaloy-4 Tubing Procurred for Fuel Cladding Research Programs, ORNL/NUREG/TM-29 (1976).

B-7.21 D. O. Hobson and C. V. Dodd, Interim Report on the Creepdown of Zry Fuel Cladding, ORNL/NUREG/TM-103 (May 1977).

B-7.22 D. O. Hobson, Quarterly Progress Report on the Creepdown and Collapse of Zircaloy Fuel Cladding for July 1976-March 1977, ORNL/NUREG/TM-125 (July 1977).

B-7.23 D. O. Hobson, Creepdown of Zircaloy Fuel Cladding - Initial Tests, ORNL/NUREG/TM-181 (April 1978).

B-7.24 D. O. Hobson, Preliminary Analysis of Surface Displacement Results in the Creepdown Irradiation Experiment HOBBIE-1, NUREG/CR-0810 and ORNL/NUREG/TM-310 (June 1979).

B-7.25 H. Stehle et al, "Uranium Dioxide Properties for LWR Fuel Rods", Nuclear Engineering and Design, 33 (1975) pp 230-260.

B-7.26 A. A. Bauer, et al., Progress on Evaluating Strength and Ductility of Irradiated Zircaloy During July through September 1975, BMI-1938 (September 1975).

B-7.27 C. Kittel, Elementary Statistical Physics, John Wiley and Sons, Inc. (1958).

7.7 Bibliography

This section is a list of additional references from the extensive literature on creep experiments. The list is reported here because one of the objectives of the MATPRO library is to provide lists of available literature for future studies of material behavior. In most cases the additional references were not used in the development of the model for creep-down because literature for the different case of creep under compressive stress has become available.

1. G. Dressler, et al., "Determination of Complete Plane Stress Yield of Zircaloy Tubing", Zirconium in Nuclear Applications, ASTM-STP-551 (1974) pp 72-103.

2. D. G. Franklin and W. A. Franz, "Numerical Model for the Anisotropic Creep of Zircaloy", Zirconium in the Nuclear Industry, ASTM-STP-633 (1977) pp 365-384.

3. P. J. Pankaskie, Irradiation Effects on the Mechanical Properties of Zirconium and Dilute Zirconium Alloys - A Review, BN-SA-618 (July 1976, updated November 1976).

4. C. E. Coleman, "Tertiary Creep in Cold-Worked Zircaloy-2", Journal of Nuclear Materials, 43 (1971) pp 180-190.

5. C. C. Busby and L. S. White, Some High Temperature Mechanical Properties of Internally Pressurized Zircaloy-4 Tubing, WAPD-TM-1243 (February 1976).

6. M. Gartner and H. Stehle, In-Pile Creep Behavior of Zircaloy-4 Cladding Tubes at 400°C, Siemens Aktiengesellschaft Reaktortechnik (September 1972).

7. M. Bernstein, "Diffusion Creep in Zirconium and Certain Zirconium Alloys", Transactions of the Metallurgical Society of AIME, 329 (1969) pp 1518-1522.

8. F. A. Nichols, "On the Mechanisms of Irradiation Creep in Zirconium-Base Alloys", Journal of Nuclear Materials, 26 (1967) pp 51-76.

9. H. P. Kreyns and M. W. Burkart, "Radiation-Enhanced Relaxation in Zircaloy-4 and Zr/2.5wt Nb/0.5 wt Cu Alloys", Journal of Nuclear Materials, 26 (1968) pp. 87-104.

10. F. L. Yagee and A. Purohit, "Biaxial Creep Characteristics of GCFR Cladding at 650° and 32.4-ksi Hoop Stress", Transactions of the American Nuclear Society, 22 (November 1975) p. 182.

11. E. F. Ibrahim and C. E. Coleman, "Effect of Stress Sensitivity on Stress-Rupture Ductility of Zircaloy-2 and Zr-2.5 wt%Nb", Canadian Metallurgical Quarterly, 12, 3 (1973) pp 285-287.

12. V. Fidleris, "The Effect of Texture and Strain Aging on Creep of Zircaloy-2" Applications of Related Phenomena for Zirconium and its Alloys, ASTM-STP-458 (1969) pp 1-17.

13. F. J. Azzarto, et al., "Unirradiated In-Pile and Postirradiation Low Strain Rate Tensile Properties of Zircaloy-4", Journal of Nuclear Materials, 30 (1969) pp 208-218.

14. W. R. Smalley, Saxton Plutonium Program: Semi Annual Progress Report for the Period Ending June 30, 1969, WCAP-3385-20 (October 1969).

15. T. E. Caye and W. R. Smalley, Saxton Plutonium Project: Quarterly Progress Report for the Period Ending December 31, 1970, WCAP-3385-26 (March 1970).

16. E. F. Ibrahim, "In-Reactor Tubular Creep of Zircaloy-2 at 260°C and 300°C", Journal of Nuclear Materials, 46 (1973) pp 196-182.

17. H. Conrad, "Experimental Evaluation of Creep and Stress Rupture", Mechanical Behavior of Materials at Elevated Temperatures, New York: McGraw-Hill Book Company, Inc., (1961) p. 149.

18. F. A. Nichols, "Theory of the Creep of Zircaloy During Neutron Irradiation", Journal of Nuclear Materials, 30 (1969) pp 249-270.

19. V. Fidleris and C. D. Williams, "Influence of Neutron Irradiation of Zircaloy-2 at 300°C", Journal of Electrochemical Technology, 4 (May - June 1966) pp 258-267.

20. E. F. Ibrahim, "In-Reactor Creep of Zirconium-2.5 Nb Tubes at 570 K", Zirconium in Nuclear Industry, ASTM-STP-551 (1974) pp 249-262.

21. C. E. Ells and V. Fidleris, "Effect of Nuetron Irradiation on Tensile Properties of the Zirconium-2.5 Weight Percent Niobium Alloy", Journal of Electrochemical Technology, 4 (May-June 1966) pp 268-274.

22. E. R. Gilbert, "In-Reactor Creep of Zr-2.5 wt Nb", Journal of Nuclear Materials, 26 (1968) pp 105-111.

23. W. J. Langford and L. E. J. Mooder, "Metallurgical Properties of Irradiated Cold-Worked of Zr-2.5 wt% Nb Pressure Tubes", Journal of Nuclear Materials, 30 (1969) pp 292-302.

24. E. F. Ibrahim, "In-Reactor Creep of Zirconium-Alloy Tubes and Its Correlation with Uniaxial Data", Applications-Related Phenomena for Zircaloy and Its Alloys, ASTM-STP-458 (1969) pp 18-36.

25. T. M. Frenkel and [illegible]. Weisz, "Effect of the Annealing Temperature on the Creep Strength of Cold-Worked Zircaloy-4 Cladding", Zirconium in Nuclear Applications, ASTM-STP-551 (1974) pp 140-144.

26. K. Kallstrom, et al., "Creep Strength of Zircaloy Tubing at 400°C as Dependent on Metallurgical Structure and Texture", Zirconium in Nuclear Applications, ASTM-STP-551 (1974) pp 160-168.

27. C. R. Woods (ed.), Properties of Zircaloy-4 Tubing, WAPD-TM-585 (December 1966).

28. O. D. Sherby and A. K. Miller, Development of the Materials Code, MATMOD (Constitutive Equations for Zircaloy), NP-567 (December 1977).

29. D. G. Franklin and H. D. Fisher, "Requirements for In-Reactor Zircaloy Creep Measurements for Application in the Design of PWR Fuel", Journal of Nuclear Materials, 65 (1977) pp 192-199.

30. W. R. Smalley, Saxton Core II Fuel Performance Evalaution Part I: Materials, WCAP-3385-56 (September 1971).

31. W. R. Smalley, Evaluation of Saxton Core III Fuel Materials Performance, WCAP-3385-57 (July 1974).

32. A. A. Bauer, et al., Progress on Evaluating Strength and Ductility of Irradiated Zircaloy During July through September 1975, BMI-1938 (September 1975).

33. A. A. Bauer, et al., Evaluating Strength and Ductility of Irradiated Zircaloy, Quarterly Progress Report, January through March 1977, BMI-NUREG-1971 (April 1977).